Cryobiology 73 (2016) 80–92

Contents lists available at ScienceDirect

Cryobiology

journal homepage: www.elsevier.com/locate/ycryo

Cryoprotectant kinetic analysis of a human articular cartilage vitrification protocol

Nadia Shardt [a], Khaled K. Al-Abbasi [b], Hana Yu [b], Nadr M. Jomha [b], Locksley E. McGann [c], Janet A.W. Elliott [a, c, *]

[a] Department of Chemical and Materials Engineering, University of Alberta, Edmonton T6G 1H9, Canada
[b] Department of Surgery, University of Alberta, Edmonton T6G 2B7, Canada
[c] Department of Laboratory Medicine and Pathology, University of Alberta, Edmonton T6G 2R7, Canada

ARTICLE INFO

Article history:
Received 29 February 2016
Received in revised form
19 May 2016
Accepted 20 May 2016
Available online 21 May 2016

Keywords:
Articular cartilage
Vitrification
Cryopreservation
Efflux
Fick's law
Diffusion

ABSTRACT

We recently published a protocol to vitrify human articular cartilage and a method of cryoprotectant removal in preparation for transplantation. The current study's goal was to perform a cryoprotectant kinetic analysis and theoretically shorten the procedure used to vitrify human articular cartilage. First, the loading of the cryoprotectants was modeled using Fick's law of diffusion, and this information was used to predict the kinetics of cryoprotectant efflux after the cartilage sample had been warmed. We hypothesized that diffusion coefficients obtained from the permeation of individual cryoprotectants into porcine articular cartilage could be used to provide a reasonable prediction of the cryoprotectant loading and of the combined cryoprotectant efflux from vitrified human articular cartilage. We tested this hypothesis with experimental efflux measurements. Osteochondral dowels from three patients were vitrified, and after warming, the articular cartilage was immersed in 3 mL X-VIVO at 4 °C in two consecutive solutions, each for 24 h, with the solution osmolality recorded at various times. Measured equilibrium values agreed with theoretical values within a maximum of 15% for all three samples. The results showed that diffusion coefficients for individual cryoprotectants determined from experiments with 2-mm thick porcine cartilage can be used to approximate the rate of efflux of the combined cryoprotectants from vitrified human articular cartilage of similar thickness. Finally, Fick's law of diffusion was used in a computational optimization to shorten the protocol with the constraint of maintaining the theoretical minimum cryoprotectant concentration needed to achieve vitrification. The learning provided by this study will enable future improvements in tissue vitrification.

1. Introduction

Osteoarthritis can be caused by progressive deterioration of articular cartilage defects/injuries. Current non-operative treatments do not affect the disease process while surgical treatments such as drilling, microfracture, autologous chondrocyte implantation, and matrix associated chondrocyte implantation have been unable to restore the normal articular cartilage architecture. Autologous osteochondral grafting can be done using multiple plugs from a different, less weight-bearing part of the joint (mosaicplasty [16]) but is limited by the amount of available articular cartilage to transplant and the risk of donor site morbidity [25]. Alternatively, fresh osteochondral allografting has shown good long term results in the management of large joint defects [7,15]. Unfortunately, fresh osteochondral allografting has become impractical due to required testing for infectious diseases and regulatory clearance before the transplantation of non-essential organs. Prolonged hypothermic storage of allografts at 4 °C has evolved to provide a storage technique prior to transplantation that enables appropriate testing. Unfortunately, storage at 4 °C for greater than 14 days has been shown to significantly decrease the cellular and physical properties of articular cartilage [8,34] and maximum storage at this temperature is 28–42 days. Thus, a long-term storage technique for articular cartilage may improve opportunities for osteochondral allografting and result in further improvement in osteochondral allografting results.

Long-term banking of biologic tissues can be accomplished

* Corresponding author. Department of Chemical and Materials Engineering, University of Alberta, Edmonton T6G 1H9, Canada.
E-mail address: janet.elliott@ualberta.ca (J.A.W. Elliott).

http://dx.doi.org/10.1016/j.cryobiol.2016.05.007

using cryopreservation, as noted in a comprehensive review of articular cartilage cryopreservation [3]. Briefly, classic cryopreservation techniques have typically used low concentrations of cryoprotectants and controlled freezing. However, many attempts at cryopreserving articular cartilage using this method failed due to cell death and matrix distortion [18,19,28]. Vitrification, the formation of an amorphous solid from an aqueous solution, has the potential to maintain matrix integrity while preserving cell viability. Preliminary studies have been performed to determine toxicity and toxicity interactions of cryoprotectants to human and porcine articular chondrocytes [6,22], permeation kinetics of cryoprotectants in articular cartilage [4,21,31], and cryoprotectant contributions to vitrifiability and vitrifiability interactions of commonly used cryoprotectants [33]. This information was used to successfully vitrify full-thickness, intact human articular cartilage on a bone base with high cell viability and preserved cellular metabolism and function [20], making long-term clinical banking of osteochondral tissue possible.

Vitrification involves the use of very high concentrations of cryoprotectants and rapid cooling rates [13] to cool the tissue below the glass transition temperature where biological and chemical reactions cease, thereby preventing cell deterioration in storage. The process of vitrification avoids the intracellular and extracellular formation of ice that is known to damage tissues [29], but the high concentrations of cryoprotectants used to vitrify tissues can also result in significant cellular toxicity. The interplay between temperature, mass transfer, and cytotoxicity was modeled by Lawson et al. [24]. The thermodynamics behind the process of vitrification was summarized by Wowk [35], examining both equilibrium and non-equilibrium vitrification methods and the physical mechanisms that underlie the formation of the amorphous solid. Past studies have also examined various cryoprotectant solutions, such as VS55, VS83, and DP6 [11,27], for the vitrification of animal articular cartilage [9,26] and tissue-engineered cartilage [14,23]. VS55 and VS83 are vitrification solutions containing a total cryoprotectant concentration of 55% (8.4 M) and 83% (12.6 M), respectively, consisting of dimethyl sulfoxide, formamide, and propylene glycol, while DP6 does not contain formamide and has a lower total cryoprotectant concentration of 6 M. As a result of the possibility for cellular damage due to toxicity, it is important to remove the cryoprotectants rapidly from the vitrified tissue upon warming.

In the clinical scenario, it is essential to remove virtually all cryoprotectants to mitigate local and systemic toxicity. Most recently, a clinical protocol was developed to remove cryoprotectants from osteochondral dowels vitrified using our 6.5 M protocol by multiple immersions in X-VIVO removal solution [36]. One objective of the current study was to investigate the kinetics of cryoprotectant efflux from intact articular cartilage after it was vitrified using our established protocol [20] by measuring the change in osmolality of the removal solution over extended periods of time. The results were compared to a theoretical model prediction using Fick's law of diffusion with previously determined diffusion coefficients for individual cryoprotectants in 2-mm thick porcine articular cartilage [4,21] and an assumption of no interaction between cryoprotectants. We hypothesized that even with various assumptions and simplifications made with the use of Fick's law, diffusion coefficients previously obtained for the permeation of individual cryoprotectants into porcine articular cartilage could be used to provide a reasonable prediction of the efflux of combined cryoprotectants from vitrified human articular cartilage.

Once the model was verified for cryoprotectant efflux calculations, a further objective was to understand the spatial distribution of individual cryoprotectants at the end of each loading step in our published protocol and use this insight to propose a shorter time for loading the cryoprotectants into the cartilage. With the shorter loading time, the minimum cryoprotectant concentrations needed for successful vitrification are still achieved within the cartilage matrix.

2. Experimental methods & materials

After ethical approval (University of Alberta Human Research Ethics Board), a hand-held coring device was used to obtain 10-mm diameter osteochondral dowels (full thickness articular cartilage on a bone base) from the non-damaged, weight bearing portion of distal femoral condyles obtained from biological discards from patients undergoing total knee arthroplasty in Edmonton, Canada. All osteochondral dowels used for this experiment appeared grossly normal to visual inspection. Patient information including age, gender, weight, height, medical diseases, and smoking status was recorded. Osteochondral dowels were placed in a Dulbecco's Phosphate Buffer Saline (PBS) solution (pH 7.1) until they were either vitrified (experimental group) or used as controls.

Osteochondral dowels were vitrified using our established protocol that results in an intended total minimum cryoprotectant concentration of 6.5 M at the bone–cartilage junction by the end of the protocol. This established protocol consists of four loading steps by immersion in solutions of: *i*) 6 M dimethyl sulfoxide (Me_2SO) for 1 h 30 min at 0 °C, *ii*) 6 M glycerol and 2.4375 M Me_2SO for 3 h 40 min at 0 °C, *iii*) 6 M propylene glycol (PG), 1.625 M glycerol, and 2.4375 M Me_2SO for 3 h at −10 °C, and *iv*) 6 M ethylene glycol (EG), 0.8125 M PG, 1.625 M glycerol, and 2.4375 M Me_2SO for 1 h 20 min at −15 °C [20]. Three vitrified osteochondral dowel samples from three patients were selected randomly for the experiment. Tubes containing the vitrified dowels were removed from liquid nitrogen and placed in a water bath at 37 °C until the solidified storage solution melted. The tubes were left in the water bath until used (time range: 5–7 min). The dowels were blot-dried using Kimwipe tissue (Kimberly-Clark, Roswell, GA), and the articular cartilage portion of each dowel was removed from its bone base using a scalpel. The volume of each articular cartilage disc was calculated using the average of thicknesses measured at three different locations.

In the experimental group, three 10-mm diameter articular cartilage discs from three males aged 64, 70 and 76 years were each immersed sequentially in two 15 mL conical centrifuge tubes (each containing 3 mL X-VIVO (Lonza, USA) at 4 °C) for 24 h. The osmolality of a 50 μl sample of the removal solution was measured with a 'μOSMETTE' micro-osmometer (Precision Systems, Natick, MA) at 0, 1, 3, 5, 10, 30, 60, 120, 180, 240, 300, 360, and 1440 min for the first immersion, and at 0, 1, 3, 5, 10, 30, 60, 120, and 1440 min for the second immersion. The extracted solution was replaced after each reading. A magnetic stirring bar (size equal to, or smaller than, 8 × 1.5 mm) was placed at the bottom of each tube to aid solution mixing with the tubes kept in a plastic rack sitting on the stirrer. After 24 h in the first tube, the articular cartilage disc was removed and dried, weighed and immersed in the second conical centrifuge tube containing 3 mL X-VIVO. Again, the change in osmolality was repeatedly measured as described previously. The articular cartilage discs were dried and weighed after the second immersion.

The experimental controls consisted of two fresh 10-mm diameter articular cartilage discs from two different donors (two females both aged 73 years). The controls were immersed in 3 mL X-VIVO without cryoprotectant loading using the same experimental protocol described for the experimental group with osmolality measurements at 0, 1, 3, 5, 10, 30, 60, and 1440 min. Unlike their experimental counterparts, the control articular cartilage discs were immersed in 3 mL X-VIVO only once (instead of twice) because there was minimal change in solution osmolality.

The measured change in osmolality (measured osmolality minus original removal solution osmolality) was normalized to the calculated volume of the articular cartilage disc (ΔOsmolality/mL dowel).

3. Governing equations for initial cryoprotectant distribution

To design a theoretical model of cryoprotectant efflux, the initial concentration profile of cryoprotectants over the entire cartilage thickness is needed, not solely the minimum concentration at the bone–cartilage junction (a criterion used during the design of the original successful vitrification protocol [20]). To determine this concentration profile, Fick's law of diffusion was used to calculate the spatial and temporal distribution of each cryoprotectant's concentration during the loading steps of the vitrification process. The cartilage was modeled as a cylindrical disc with thickness a and radius R_c, and a two-dimensional form of Fick's law was used [10]:

$$\frac{\partial C}{\partial t} = D\left(\frac{\partial^2 C}{\partial x^2} + \frac{\partial^2 C}{\partial r^2} + \frac{1}{r}\frac{\partial C}{\partial r}\right), \tag{1}$$

where C is concentration, t is time, x is position in the axial direction, r is position in the radial direction, and D is the diffusion coefficient. Fig. 1 illustrates the geometry of a cartilage disc attached to bone for the loading protocol with a 2-D slice through its center. Concentration was calculated over $0 \le x \le a$ and $0 \le r \le R_c$ for time up to the end of each loading step.

For numerical computation, mesh independence was tested, and a mesh was constructed using a Delaunay triangulation algorithm with a chosen maximum triangle edge length of 0.05 mm. The built-in MATLAB® (ver. 7.12, Natick, MA, USA) parabolic partial differential equation solver *parabolic()* was used to calculate the concentration profile of each cryoprotectant separately at the end of every loading step of the protocol. Within the *parabolic()* function, the time step is set to achieve a relative error less than 10^{-6}.

3.1. Initial conditions

For the first loading step, it was assumed that the cartilage initially had a cryoprotectant concentration of 0 M throughout. The concentration profile of Me_2SO in the cartilage after 1 h 30 min was then used as the initial condition for the second loading step. Similarly, the concentration profiles of Me_2SO and glycerol after 3 h 40 min were taken to be initial conditions for the third loading step, and finally the concentration profiles of each cryoprotectant after the 3 h of the third loading step were used as initial conditions for the fourth loading step.

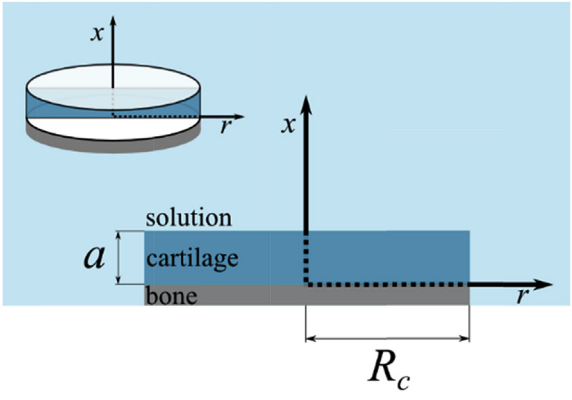

Fig. 1. Schematic of a 2-D slice through a cartilage disc with thickness a and radius R_c attached to bone and immersed in a cryoprotectant solution.

3.2. Boundary conditions

The cartilage segment of the osteochondral dowel has four boundary conditions; the first is at the bone–cartilage junction where we assumed no flow of cryoprotectants. That is,

$$\left.\frac{\partial C}{\partial x}\right|_{x=0} = 0. \tag{2}$$

The second boundary condition is at the center of the cylinder ($r = 0$) where there is no flow due to symmetry. The third boundary condition is the concentration of the surrounding solution at the surface of the cartilage in the axial direction ($x = a$), and the final boundary condition is the concentration of the surrounding solution at the surface of the cartilage in the radial direction ($r = R_c$).

3.3. Assumptions

Fick's law assumes that the solution is ideal and dilute and does not account for water movement during cryoprotectant diffusion, which results in an underestimate of actual concentrations observed during loading when compared to more complex models of transport mechanisms and experimental data [1,2,5]. Extensive experimental work would be needed using a large number of precious human samples in order to implement a more sophisticated model [1,2,5], since parameters such as the permeability of each cryoprotectant would need to be determined. Fick's law, particularly when effective diffusion coefficients are obtained by fitting actual experimental data (that has water transport occurring) as is the case for the diffusion coefficients used here, provides useful insight into the general trends of cryoprotectant diffusion into cartilage and, because it underestimates, provides a means for conservative design of protocols.

Using the activation energy (E_a) and prefactors (A) determined in our previous work for porcine cartilage [4,21,31], the diffusion coefficients to be used for human articular cartilage at the outlined temperatures can be calculated using the Arrhenius expression (Equation (3))

$$D = A\exp\left(\frac{E_a}{RT}\right), \tag{3}$$

where R is the universal gas constant and T is the absolute temperature. Table 1 lists the values of E_a and A for each cryoprotectant used.

4. Governing equations for efflux

Based on the concentration profile of the cryoprotectants throughout the entire cartilage at the end of the loading protocol, a theoretical prediction of cryoprotectant efflux can be made. Fick's law (Equation (1)) is used to determine how the concentration of each cryoprotectant changes as a function of position for $0 \le x \le a$ and $0 \le r \le R_c$ and as a function of time for $0 \le t \le 24$ h. The initial condition for efflux is each cryoprotectant's individual concentration profile as calculated at the end of the fourth loading step. The boundary condition at the surface is the concentration of each cryoprotectant in the surrounding X-VIVO solution. At $t = 0$, this concentration is 0 M for each cryoprotectant. The boundary and initial conditions are updated for each cryoprotectant every 5 min. Efflux predictions were also made for shorter time steps, and 5 min was chosen to accurately capture the dynamic process of efflux while reducing computational time. The number of moles of each

Table 1
Pre-exponential factor, activation energy, and osmotic virial coefficients of each cryoprotectant from Ref. [4] and Ref. [37].

Cryoprotectant	A (m^2/s) [4]	E_a (kcal/mol) [4]	B_i ($molal^{-1}$) [37]	C_i ($molal^{-2}$) [37]
Me_2SO	2.9895×10^{-7}	3.9 ± 1.6	0.108 ± 0.005	0
Glycerol	2.0803×10^{-6}	5.6 ± 1.2	0.023 ± 0.001	0
PG	1.6971×10^{-5}	6.63 ± 0.04	0.039 ± 0.001	0
EG	1.833×10^{-7}	3.8 ± 0.7	0.020 ± 0.001	0

cryoprotectant in the X-VIVO solution is calculated numerically using

$$n_{CPA,XVIVO}(t) = 0.776 \times \int_0^{2\pi}\int_0^{R_c}\int_0^{a} [C_{CPA}(x,r,0) - C_{CPA}(x,r,t)]dx\,dr\,d\theta, \quad (4)$$

where R_c is the radius of the cartilage, a is the thickness, C_{CPA} denotes the concentration profile of each cryoprotectant in the cartilage, and $n_{CPA,XVIVO}$ is the number of moles of each cryoprotectant in the X-VIVO solution. The factor of 0.776 is the percent of isotonic cartilage volume made up of solution and therefore capable of holding the cryoprotectants [21,31]. The concentration of each cryoprotectant in the solution was determined by dividing the moles by the X-VIVO solution volume (3 mL).

In this study, the cartilage disc radius was 5 mm and the thicknesses for Samples 1, 2, and 3 were 2.98 mm, 2.12 mm, and 2.08 mm, respectively. The diffusion coefficients from our previous work on porcine articular cartilage for the cryoprotectants at 4 °C (Table 1) were used when solving Equation (1) for efflux [4,21,31]. The molalities of the cryoprotectants in the X-VIVO solution were calculated individually by dividing the moles by the mass of the X-VIVO (assuming a density of 1 g/mL). After determining the molality of each cryoprotectant present in the X-VIVO solution, the form of the osmotic virial equation proposed by Elliott et al. [12,30] was used to calculate osmolality:

$$\pi = \sum_i m_i + \sum_i \sum_j \frac{B_i + B_j}{2} m_i m_j + \sum_i \sum_j \times \sum_k (C_i C_j C_k)^{1/3} m_i m_j m_k, \quad (5)$$

where π is the osmolality (osmol/kg solvent), B_n and C_n are solute-specific virial coefficients, and m_n are molalities (moles solute/kg solvent) for each of the n components. The solute-specific virial coefficients for Me_2SO, glycerol, PG, and EG are those recently updated by Zielinski et al. [37], as listed in Table 1. The osmolality predicted for each sample was then normalized to the volume of the articular cartilage disc.

5. Governing equations for optimization

We chose a cartilage sample with a thickness of 2.00 mm as a representative size for analyzing kinetics towards reducing the time needed for the vitrification protocol because this is a common thickness for femoral articular cartilage. The surface area of articular cartilage defects can range from 0.5 cm^2 to 12 cm^2 [17]. Due to this variation, it is planned to bank entire condyles; therefore we use a 1-D representation of the cartilage as a slab to optimize the protocol and ensure successful vitrification of large area banked tissue, which will be processed after warming for any surface area that may be encountered in a clinical setting.

The 1-D representation of Fick's law is

$$\frac{\partial C}{\partial t} = D\frac{\partial^2 C}{\partial x^2} \quad (6)$$

where the boundary conditions include the concentration of the surrounding solution at $x = 2.00$ mm and the no flow condition at the bone–cartilage junction ($x = 0$ mm) given by Equation (2). Fig. 2 illustrates the geometry used for shortening the loading steps of the vitrification protocol. The cartilage is modeled as a slab with 2.00-mm thickness attached to bone placed in a cryoprotectant solution.

Successful vitrification can only occur if each of the loading steps takes place at a temperature above the freezing point of the solution in the articular cartilage. The freezing point can be calculated using [30]

$$T_{FP}^0 - T_{FP} = \frac{\left[W_1 \Big/ \left(\overline{s_1^{0L}} - \overline{s_1^{0S}}\right)\right] R T_{FP}^0 \pi}{1 + \left[W_1 \Big/ \left(\overline{s_1^{0L}} - \overline{s_1^{0S}}\right)\right] R\pi} \quad (7)$$

where T_{FP}^0 is the freezing point of pure water (273.15 K), T_{FP} is the freezing point of the solution (K), W_1 is the molar mass of water (0.01802 kg/mol), $\overline{s_1^{0L}}$ and $\overline{s_1^{0S}}$ are the molar entropies of pure liquid water and of pure water in the solid phase, respectively ($\overline{s_1^{0L}} - \overline{s_1^{0S}} = 22.00$ J/mol K), R is the universal gas constant (8.314 J/mol K), and π is osmolality of the solution (osmol/kg solvent). The osmolality π is calculated using Equation (5), where m_i (mol solute/kg solvent) are calculated as a function of water density and cryoprotectant molar concentration, molar mass, and density. Osmolality varies as a function of distance from the solution boundary, and thus the freezing point temperature will also vary.

6. Experimental results

Three vitrified osteochondral dowels and two fresh control dowels from 5 different patients were used with average articular cartilage thicknesses of the three vitrified dowels being 2.98 mm, 2.12 mm, and 2.08 mm (Samples 1, 2, and 3), respectively. Results for cryoprotectant efflux during the first and second immersions for the experimental group are shown in Fig. 3. In the first immersion, the initial rate of change in osmolality of the removal solution per

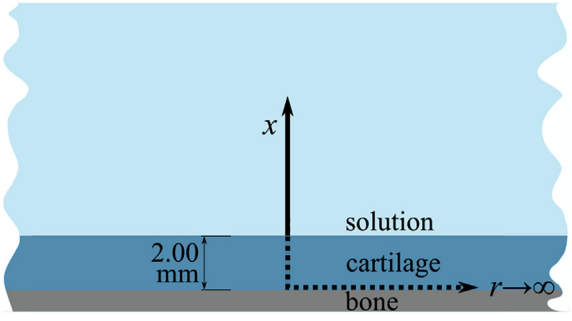

Fig. 2. Schematic of a 1-D slab with 2.00-mm thickness and infinite radius.

dowel volume of all three vitrified dowels was rapid. Subsequently, the rate of change in osmolality slowed with time until a plateau was reached. This recurred in the second immersion but with a smaller change in osmolality and a lower plateau. The plateau was considered to be reached when the change in osmolality of the removal solution was less than the change in osmolality of the control samples. Immersing the fresh dowels from the control group resulted in minimal changes in the osmolality of the removal solution (0–27 mOsmol/(kg mL)).

7. Theoretical results

7.1. Concentration profiles

Contour plots of the calculated concentration profiles using the 2-D model for each of the four loading steps of the DGPE vitrification protocol are shown in Fig. 4 for an articular cartilage disc thickness of 2.00 mm. These profiles illustrate the variation in concentration as a function of radius and thickness for a slice through the center of the cartilage dowel. Figs. 5–7 show the calculated concentration profile using the 2-D theoretical model as a function of thickness at $r = 0$ for Samples 1, 2, and 3, respectively.

7.2. Average concentrations

The concentrations of each cryoprotectant averaged over the entire cartilage dowel using the 2-D model for Samples 1 to 3 at the end of the fourth loading step are summarized in Table 2. The average total concentration of cryoprotectants over the whole dowel at the end of the fourth loading step is also listed for each sample. Table 3 shows the total concentration of cryoprotectants at the surface, middle, and bone–cartilage junction for Samples 1 to 3 at the center of the cartilage dowel ($r = 0$) after the fourth loading step using the 2-D model.

7.3. Theoretical efflux

The theoretical predictions of the cryoprotectant efflux process are shown in Figs. 8 and 9. Note that the cartilage discs had been removed from the bone before immersion in the removal solution for the efflux experiments, and efflux therefore occurs from both surfaces at $x = 0$ and $x = a$ and this was taken into consideration in efflux calculations. Fig. 8 illustrates how the cryoprotectants diffuse out of Sample 1 in the first immersion at $r = 0$. The spatial concentration profile of each cryoprotectant inside the cartilage is shown at times of 1 min, 5 min, 10 min, and 30 min. In Fig. 9, the theoretical efflux of each cryoprotectant from Sample 1 for the first immersion is plotted. The total change in osmolality per volume of dowel was predicted using Equation (5) and is illustrated by the solid line.

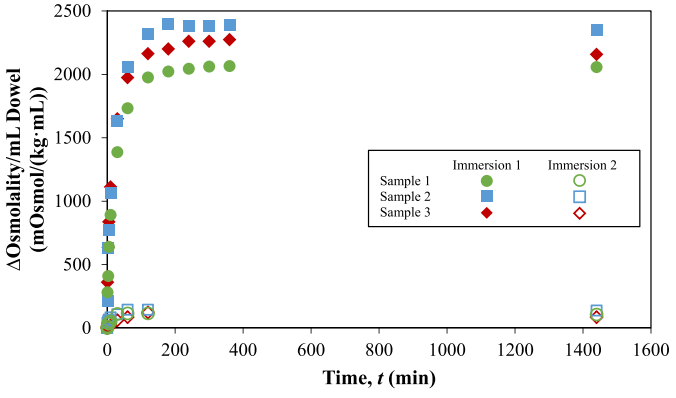

Fig. 3. Change in osmolality of the removal solution, normalized to the articular cartilage disc volume, during the first and second immersions of the experiment for three samples.

As seen in Fig. 10(a–c), the solid line represents the theoretical prediction of the total cryoprotectant efflux from cartilage discs as calculated according to Fick's law of diffusion. The data points show the experimentally measured values of osmolality in the X-VIVO solution. The percentage error between the final amount of cryoprotectants effluxed in the experiment and the expected amount as predicted by the theoretical model is shown in Table 4 for each of the three samples.

8. Theoretical shortening of the vitrification protocol

In the original protocol [20], each loading step was designed to individually achieve the targeted minimum concentration of the cryoprotectant at the bone–cartilage junction. The original protocol's concentration (Equation (6)) and freezing point temperature (Equation (7)) profiles can be seen in Fig. 11(a–d) for a cartilage thickness of 2.00 mm using the 1-D representation of Fick's law. In the first loading step, the Me_2SO reaches 2.4 M at the bone–cartilage junction, and the concentration gradually increases closer to the cartilage–solution boundary. As the cartilage is placed in the second loading solution containing a maintenance concentration of Me_2SO, the concentration profile flattens, and for the remaining loading steps, a relatively uniform profile of Me_2SO is observed. We can take advantage of this equilibrating process that occurs over the second to fourth loading steps to shorten the time needed for the first loading step and in fact, remove this step entirely, as seen in the shortened protocol proposed below. Similarly, we can shorten the time needed for the second and third loading steps due to the equilibration of glycerol and PG that occurs over the subsequent steps. To achieve this shortening, Fick's law will be used in 1-D for a 2-mm thick cartilage sample to permit the successful vitrification of a wide range of cartilage surface areas.

In addition to cryoprotectant concentration, an appropriate temperature for each loading step of a successful vitrification protocol must be determined. In the original protocol consisting of four loading steps, the temperatures were 0 °C, 0 °C, −10 °C, and −15 °C, respectively. The temperatures of the third and fourth steps were chosen to be 2 °C greater than the freezing point temperature at the bone–cartilage junction in the previous step so that ice formation is avoided. For the first iteration of optimization, we consider the same temperatures as used in the original protocol for each loading step.

As outlined in the original protocol [20], the minimum total cryoprotectant concentration needed for successful vitrification is 6.5 M. Due to the toxicity and toxicity interactions of cryoprotectants, this total 6.5 M concentration was split between 2.4375 M Me_2SO, 1.625 M glycerol, 0.8125 M PG, and 1.625 M EG, and it is these individual concentrations that are desired for the shortened protocol. Since each consecutive loading step impacts the final concentration profile of the first three loaded cryoprotectants, the last step is optimized first. For the fourth loading step, a time of 140 min is needed to achieve at least 1.625 M EG at the bone–cartilage junction. This was calculated by iteratively increasing the time by 10 min.

Since the equilibration of Me_2SO is rapid, the concentration of the original first loading step is decreased from 6 M to 3 M Me_2SO for the optimization calculations. The first three loading steps were given all possible times between 30 min and 230 min in MATLAB, and the combinations of times that yield a total cryoprotectant concentration greater than 6.5 M at the bone–cartilage junction

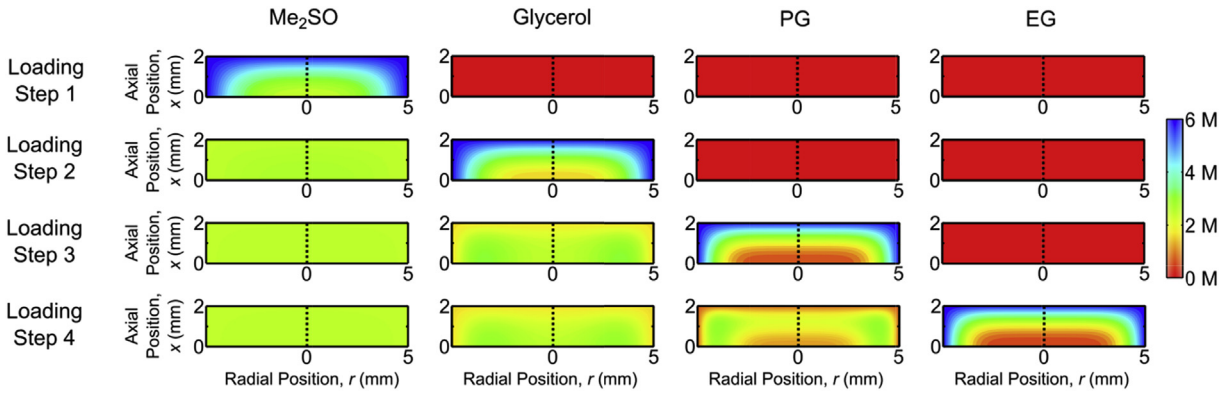

Fig. 4. Contour plots of the concentration distribution as a function of thickness and radius calculated for a cartilage disc with $a = 2$ mm and $R_c = 5$ mm for the original vitrification protocol at the end of each loading step for Me_2SO, glycerol, PG, and EG using the 2-D model.

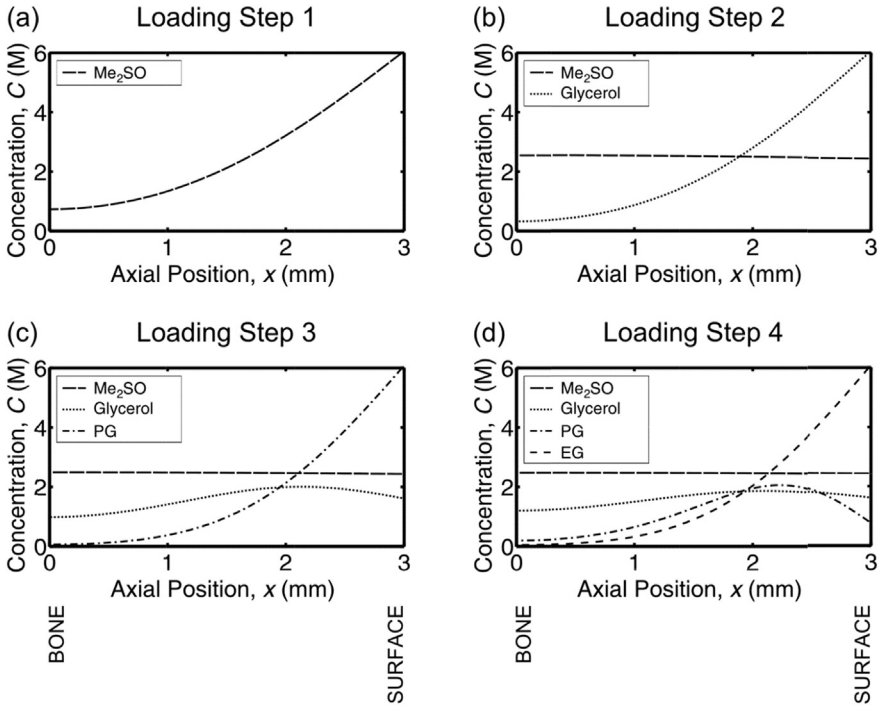

Fig. 5. Concentration profiles calculated using the 2-D model for the loading of Sample 1 (2.98 mm thick) at $r = 0$; (a) the concentration distribution of Me_2SO over the thickness of the dowel after the first loading step time of 1 h 30 min. (b) the distribution of Me_2SO and glycerol after the second loading step time of 3 h 40 min. (c) the distribution of Me_2SO, glycerol, and PG after the third loading step time of 3 h. (d) the distribution of Me_2SO, glycerol, PG, and EG after the fourth loading step time of 1 h 20 min.

were identified. Out of these identified combinations, those with individual concentrations greater than 2.3 M Me_2SO, 1.5 M glycerol, and 0.7 M PG were selected, so that the values were close to the previously outlined 2.4375 M Me_2SO, 1.625 M glycerol, and 0.8125 M PG. Several possible combinations of times satisfied these requirements with a minimum total loading time of 7 h 20 min. The calculated first loading step times were at the lower end of the examined range (30–40 min), and any further decrease of this amount could be balanced by increasing the time of the second loading step since the temperature remains constant between these two loading steps. Ultimately, the first loading step could be removed. Since the Me_2SO concentration in the second solution is only 2.4375 M and not the 3 M of the optimized first loading solution, an extra 10 min was needed for the second solution to ensure that a minimum of 2.3 M Me_2SO was present at the bone–cartilage junction by the end of the last step.

A total loading time of 7 h 30 min was needed to achieve the desired minimum individual and total cryoprotectant concentrations if the first loading step was removed. After the first iteration of optimization, the vitrification protocol consisted of three loading steps: *i*) a solution of 2.4375 M Me_2SO and 6 M glycerol for 3 h 30 min at 0 °C, *ii*) a solution of 2.4375 M Me_2SO, 1.625 M glycerol, and 6 M PG for 1 h 40 min at −10 °C, and *iii*) a solution of 2.4375 M Me_2SO, 1.625 M glycerol, 0.8125 M PG, and 6 M EG for 2 h 20 min at −15 °C. However, the freezing point temperature at the bone–cartilage junction was not depressed sufficiently for the second and third loading steps to take place at −10 °C and −15 °C, respectively. As a result, the temperature of these loading steps must be increased. This temperature increase will accelerate the diffusion process, and this means that the time of the process can be further reduced. Temperatures that were 2 °C above the freezing point at the bone–cartilage junction were selected for the second

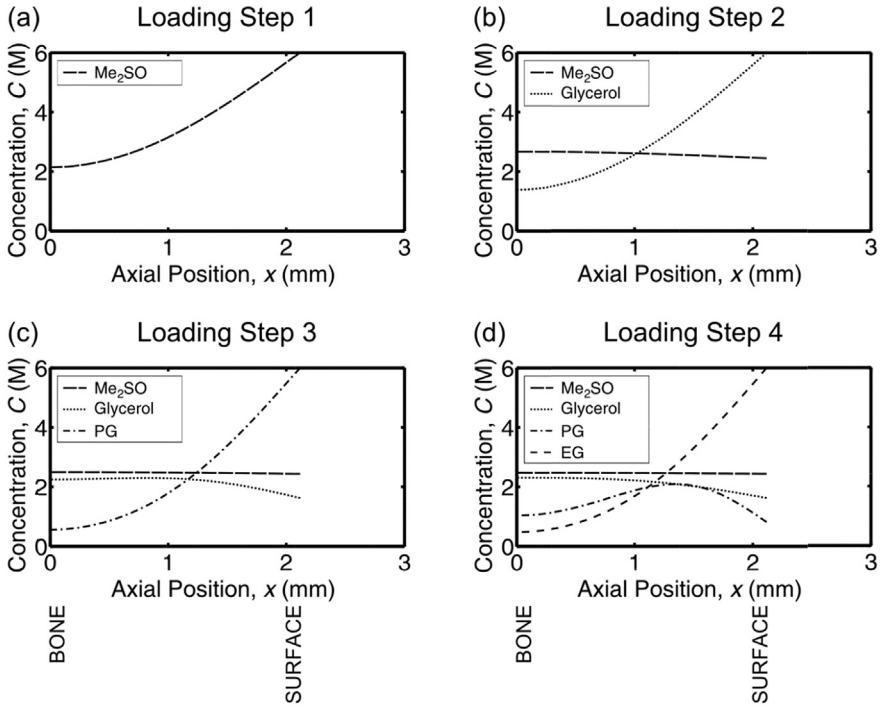

Fig. 6. Concentration profiles calculated using the 2-D model for the loading of Sample 2 (2.12 mm thick) at $r = 0$; (a) the concentration distribution of Me_2SO over the thickness of the dowel after the first loading step time of 1 h 30 min. (b) the distribution of Me_2SO and glycerol after the second loading step time of 3 h 40 min. (c) the distribution of Me_2SO, glycerol, and PG after the third loading step time of 3 h. (d) the distribution of Me_2SO, glycerol, PG, and EG after the fourth loading step time of 1 h 20 min.

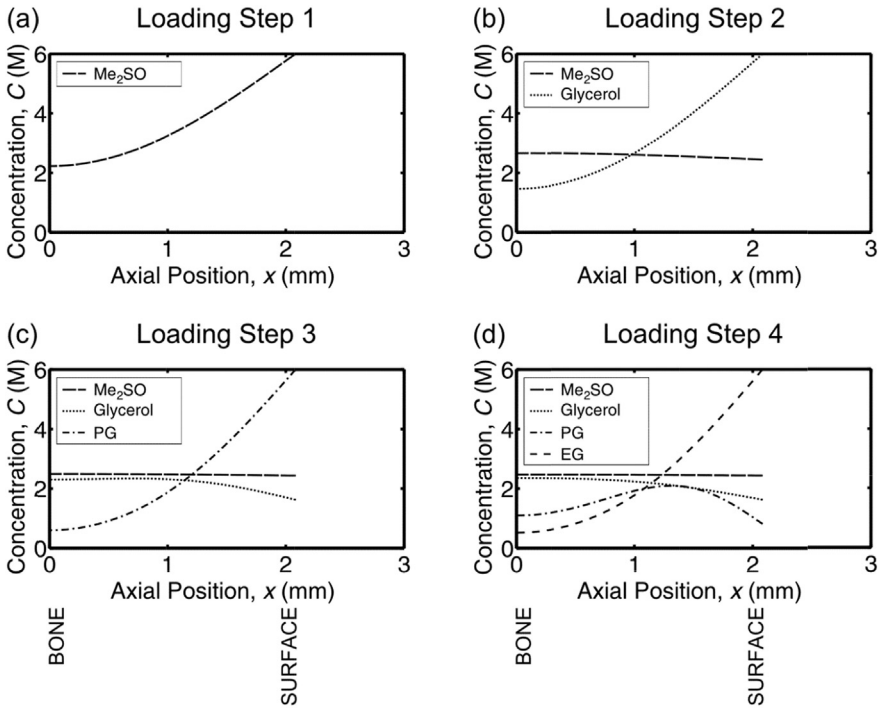

Fig. 7. Concentration profiles calculated using the 2-D model for the loading of Sample 3 (2.08 mm thick) at $r = 0$; (a) the concentration distribution of Me_2SO over the thickness of the dowel after the first loading step time of 1 h 30 min. (b) the distribution of Me_2SO and glycerol after the second loading step time of 3 h 40 min. (c) the distribution of Me_2SO, glycerol, and PG after the third loading step time of 3 h. (d) the distribution of Me_2SO, glycerol, PG, and EG after the fourth loading step time of 1 h 20 min.

and third loading steps, and the previously outlined optimization process was carried out to achieve the desired minimum cryoprotectant concentrations at these new temperatures. After this optimization, the chosen temperatures were confirmed to still be adequate for vitrification (i.e. 2 °C greater than the freezing point at the bone–cartilage junction).

The final optimized vitrification protocol consists of three loading steps *i*) a solution of 2.4375 M Me_2SO and 6 M glycerol for

Table 2
Calculated concentration (M) of cryoprotectants averaged over the entire cartilage disc after loading step 4 of the original vitrification protocol for all samples.

Cryoprotectant	Me_2SO (M)	Glycerol (M)	PG (M)	EG (M)	Average total cryoprotectant concentration (M)
Sample 1 2.98 mm	2.42	2.01	1.74	2.89	9.06
Sample 2 2.12 mm	2.43	2.21	1.97	3.38	9.99
Sample 3 2.08 mm	2.41	2.21	1.98	3.36	9.96

Table 3
Calculated total concentration (M) of cryoprotectants at the surface, middle, and bone–cartilage junction for $r = 0$ after loading step 4 of the original protocol for all cartilage discs.

	Total cryoprotectant concentration at surface for $r = 0$ (M)	Total cryoprotectant concentration at middle for $r = 0$ (M)	Total cryoprotectant concentration at bone for $r = 0$ (M)
Sample 1 2.98 mm	10.88	6.36	3.92
Sample 2 2.12 mm	10.88	8.52	6.30
Sample 3 2.08 mm	10.88	8.53	6.44

3 h 30 min at 0 °C, *ii*) a solution of 2.4375 M Me_2SO, 1.625 M glycerol, and 6 M PG for 1 h 30 min at −7 °C, and *iii*) a solution of 2.4375 M Me_2SO, 1.625 M glycerol, 0.8125 M PG, and 6 M EG for 2 h at −10 °C.

The optimization results in a vitrification protocol that is 2.5 h shorter yet maintains the minimum concentration previously shown to result in successful vitrification [20] throughout the cartilage matrix and reduces the possibility of ice formation with an appropriate selection of loading step temperatures. This is a theoretical vitrification protocol that has not been proven to maintain cell viability. Fig. 11 shows the concentration profiles for the original and modified loading steps and the predicted freezing point temperatures as calculated by the 1-D model. The shorter times identified from this 1-D optimization were then used to predict the concentration contours for a 2-D cartilage disc with a 2-mm thickness and 5-mm radius, as shown in Fig. 12. The modified protocol in Fig. 12 can be directly compared with the original protocol in Fig. 4. Table 5 summarizes the desired cryoprotectant concentrations with the bone–cartilage junction concentrations of each cryoprotectant for the original and the modified protocols. For the modified protocol, it can be seen that the final concentrations of Me_2SO, glycerol, PG, and EG at the bone–cartilage junction are close to the desired values, and the total cryoprotectant concentration is greater than the minimum 6.5 M needed for successful vitrification.

9. Discussion

Understanding the kinetics of cryoprotectant loading and efflux into and out of intact articular cartilage is valuable information for designing loading and unloading steps during the process of preparing vitrified cartilage tissue for subsequent transplantation.

Our previously published vitrification protocol [20] was designed specifically using permeation kinetics for individual cryoprotectants determined in pig articular cartilage permeation studies [4,21,31]. The diffusion coefficients were assumed to be reasonable approximations of those for human articular cartilage and were used to estimate the exposure times required during the vitrification protocol to get the desired concentration of each cryoprotectant at the bone–cartilage junction of the tissue to be vitrified. The times were based on calculations performed for 2-mm thick articular cartilage. These assumptions proved to be practically useful as we have been able to use this information to successfully vitrify human articular cartilage [20]. In the current study, we endeavored to verify that reasonable predictions of efflux from vitrified human articular cartilage could be made using a number of simplifying assumptions: *i*) diffusion coefficients measured from permeation experiments could be used to predict efflux, *ii*) diffusion coefficients measured for individual cryoprotectants could be used to predict diffusion of combined cryoprotectants, *iii*) diffusion coefficients measured for porcine articular cartilage could be used to make predictions for human articular cartilage of various thicknesses, and *iv*) simplifying the diffusion calculations by using Fick's law would not lead to large errors.

In the experiments, as expected, there was an initial rapid efflux of the cryoprotectants out of the tissue after immersion in the washing solution that slowed with time. A small amount of the cryoprotectants remained even after the initial 24 h and was removed with the second wash. This remaining cryoprotectant within the tissue even after 24 h supports our recommended method of clinical cryoprotectant removal using multiple short washes with fresh washing solution [36].

The theoretical prediction of cryoprotectant efflux from human articular cartilage after the tissue had come to equilibrium with the first immersion solution agreed with the measured amount within a maximum of 15% error (Fig. 10 and Table 4). The predicted efflux in the first immersion for each sample was greater than the amount effluxed experimentally. This means that the theoretically-calculated cryoprotectant concentration profile initially in the cartilage (or equivalently, at the end of the loading steps in the vitrification protocol) is greater in magnitude than the actual concentration profile within the cartilage disc. This is unexpected because the theoretical model of Fick's law is known to underestimate the actual permeation of cryoprotectants in porcine articular cartilage [1]. The fact that the theoretical model overestimates experimental efflux measurements therefore suggests that the effective Fick's law diffusion coefficients for cryoprotectants in porcine articular cartilage are greater than the Fick's law diffusion coefficients in human cartilage; this conclusion is supported by experimental evidence that the permeability of human articular cartilage is lower than that of porcine articular cartilage [32]. In addition to the different mechanical properties of porcine and

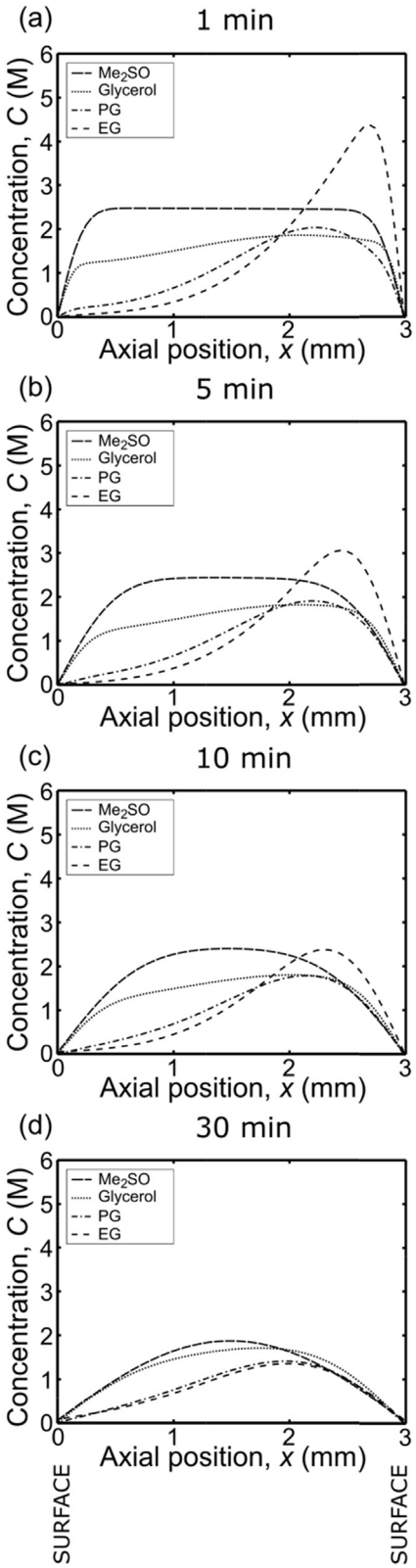

Fig. 8. Cryoprotectant concentration calculated using the 2-D model inside the cartilage disc during efflux as a function of axial position at $r = 0$ in Sample 1 at times of (a) 1 min, (b) 5 min, (c) 10 min, and (d) 30 min during the first immersion.

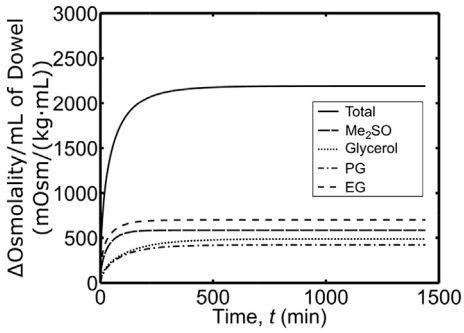

Fig. 9. Breakdown of cryoprotectant efflux from Sample 1 for the first immersion.

human articular cartilage, diffusion coefficients may change for different thicknesses of cartilage since cartilage is not a homogenous structure. As the cartilage thickness changes, the distributions of its constituents vary and may result in different diffusion coefficients.

To enhance the understanding of what is happening within the cartilage matrix, spatial distributions of cryoprotectant concentrations within the cartilage matrix after each step of our original vitrification process were calculated using Fick's law of diffusion and are shown in Figs. 5–7. The final concentration at the bone–cartilage junction will vary depending on the thickness of the cartilage because the permeation times in the protocol were determined specifically for a standard 2-mm thick tissue as opposed to custom designed for each sample. Thus, the 2.98-mm thick tissue will have less than 6.5 M total cryoprotectant concentration at the bone–cartilage junction, while the 2.12-mm and 2.08-mm thick samples have concentrations close to 6.5 M at the bone–cartilage junction (Table 3). In addition, cryoprotectant concentrations spatially averaged over the whole tissue were calculated at the end of the fourth loading step and are given in Table 2. Designing the loading protocol to achieve 6.5 M total cryoprotectant concentration at the bone–cartilage boundary results in a substantially higher overall cryoprotectant concentration at the end of loading due to the spatial inhomogeneity of the diffusion driven loading process.

At the cartilage surface, the last cryoprotectant to be added (EG) remains at its initial loading concentration (6 M) at the cartilage surface, with concentration reducing as the depth increases. Even though the third cryoprotectant to be added (PG) is at the final solution concentration at the cartilage surface, just 1 mm in from this surface, the concentration remains higher than designed because of insufficient time to equilibrate. The concentration of glycerol throughout the cartilage thickness becomes progressively higher from the cartilage surface to the bone–cartilage junction and is consistently greater than the designed concentration. These observations could have important ramifications during the vitrification process. The high cryoprotectant concentrations at the surface in all samples leave the cells in these areas at higher risk for cryoprotectant toxicity. This is in effect until a depth of approximately 1 mm where the concentrations are progressively lower. At the bone–cartilage junction, if the tissue is close to 2 mm thick, it can be assumed that the total cryoprotectant concentration is close to 6.5 M. But, as the tissue increases in thickness, the concentration at the bone–cartilage junction will decrease, leaving cells in this area at risk for ice formation during the cooling or warming process. The "average" concentrations shown in Table 2 can be misleading. All samples had an average total cryoprotectant concentration greater than the 6.5 M targeted for 2-mm thick cartilage samples. This was because the cryoprotectant concentration was just slightly below 6.5 M at the bone–cartilage junction for each experimental sample, while the cryoprotectant concentration

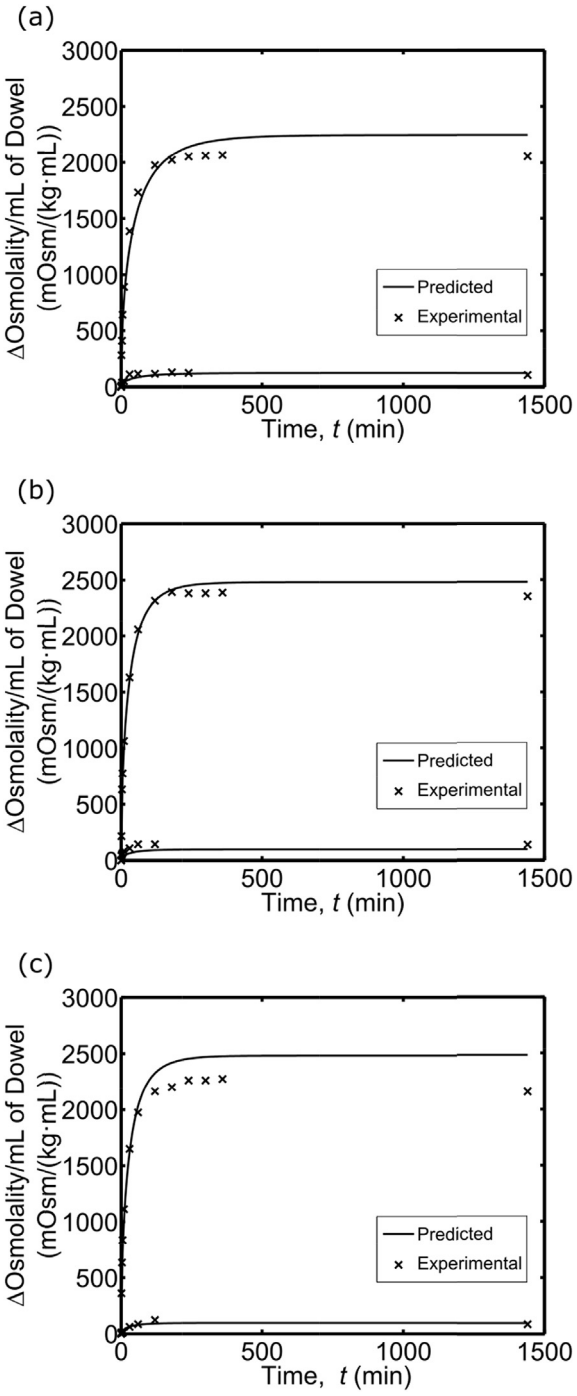

Fig. 10. Predicted and experimental efflux of all cryoprotectants from (a) Sample 1, (b) Sample 2, and (c) Sample 3 with thicknesses of 2.98 mm, 2.12 mm, and 2.08 mm, respectively.

nearer to the surface was much higher than 6.5 M. Table 3 summarizes the total cryoprotectant concentrations at the surface, in the middle of the tissue, and at the bone–cartilage junction for each sample.

The issue of toxicity is paramount due to the high cryoprotectant concentration in the cartilage closest to the solution, and this is addressed with the new shorter vitrification protocol presented herein. This shortened version has not been proven to be effective at maintaining cell viability but demonstrates that nearly equivalent concentrations can be achieved at the bone-cartilage junction in a significantly shorter time period. The excess PG shown in Fig. 11(d) above the minimum 0.8125 M is reduced in the modified shorter protocol. Fig. 11(g) shows that by the end of the modified last loading step, the concentration profile of PG is relatively uniform at the targeted value of 0.8125 M. The final spatial distributions of Me_2SO, glycerol and EG are relatively unchanged, but the cells closer to the solution are still exposed to high concentrations of cryoprotectant over the duration of the protocol. However, it is important to note that decreasing the duration of the loading steps lowers the risk of toxic exposure of the cells to the cryoprotectants. The removal of the first loading step further decreases toxicity risk since the exposure to 6 M Me_2SO has been eliminated, while still achieving a 2.3 M Me_2SO concentration by the end of the protocol. The overall effect is a decrease in cryoprotectant exposure and a maintenance of the minimum total 6.5 M cryoprotectant concentration throughout the articular cartilage, as summarized in Table 5.

10. Conclusions

This study suggests that the permeation and efflux kinetics of cryoprotectants in human articular cartilage are similar to those in porcine articular cartilage. The permeation and efflux of cryoprotectants into and out of articular cartilage during the vitrification process is complex with spatially and temporally varying concentrations throughout the matrix that could have important effects on the cell viability. Transport simulations are a key tool in understanding the kinetics of permeation and efflux, and this may help in optimizing cryoprotectant addition and removal processes. The optimization methods outlined in this study can be extended to other cryoprotectant solutions and multi-step vitrification procedures for other biologic tissues if the mass transfer properties of the cryoprotectant solution in the structure are known.

Previous work developed a vitrification protocol based on criteria of cryoprotectant concentration, cryoprotectant toxicity, and freezing point temperature; it was successful when tested on intact human articular cartilage [20]. The current study shortened this protocol by 2.5 h while still achieving the minimum necessary cryoprotectant concentration at the bone–cartilage junction as outlined in the established protocol and taking place at appropriate temperatures that are predicted to avoid ice formation. It should be clearly stated that the effectiveness of this shortened protocol is

Table 4
The percentage error between the theoretical predictions and the experimental results for the three samples (cartilage discs excised from bone) at the end of the first immersion.

	Theoretical 24 h (mOsm/(kg mL))	Experimental 24 h (mOsm/(kg mL))	Percentage error (%)
Sample 1 2.98 mm	2245	2057	9.1
Sample 2 2.12 mm	2481	2352	5.5
Sample 3 2.08 mm	2482	2157	15.1

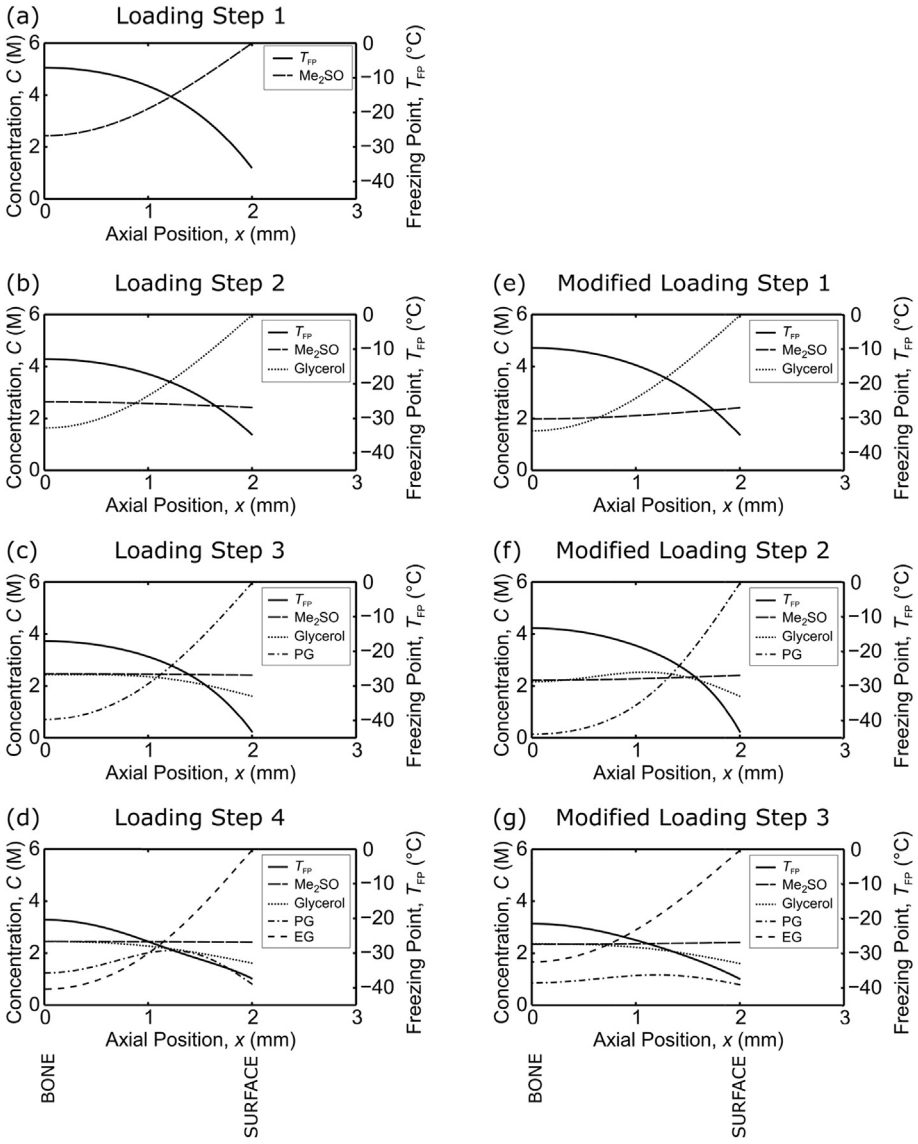

Fig. 11. Concentration profiles and freezing point temperature profiles calculated at the end of each loading step for a 2-mm slab using the 1-D model for the original vitrification protocol (*a*–*d*) and the new shortened vitrification protocol (*e*–*g*); (e) the distribution of Me_2SO and glycerol after the modified first loading step time of 3 h 30 min at 0 °C. (f) the distribution of Me_2SO, glycerol, and PG after the modified second loading step time of 1 h 30 min at −7 °C. (g) the distribution of Me_2SO, glycerol, PG, and EG after the modified third loading step time of 2 h at −10 °C.

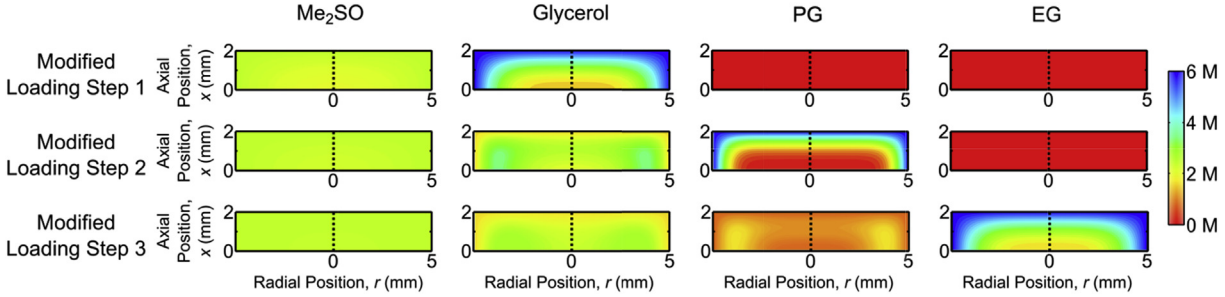

Fig. 12. Contour plots of the concentration distribution as a function of thickness and radius calculated for a cartilage disc with $a = 2$ mm and $R_c = 5$ mm for the shortened vitrification protocol at the end of the modified loading steps for Me_2SO, glycerol, PG, and EG. These plots were calculated by using the 2-D model with the shorter times previously identified in the 1-D optimization.

Table 5
Calculated cryoprotectant concentrations (M) at the bone–cartilage junction at $r = 0$ after the end of the original cryoprotectant loading protocol and after the end of the modified shortened loading protocol for a 2-mm thick cartilage disc with $R_c = 5$ mm as calculated by the 2-D model.

Cryoprotectant	Bone–Cartilage junction concentration		
	Desired (M)	Original protocol (M)	Modified protocol (M)
Me_2SO	2.4375	2.46	2.37
Glycerol	1.625	2.47	2.39
PG	0.8125	1.25	0.88
EG	1.625	0.63	1.69
Total	6.50	6.81	7.33

theoretical at this time and has not been shown to provide similar results to the previously described protocol. If this shortened protocol proves to be clinically effective, it would decrease the time needed for vitrification from 9.5 h to 7 h; this is significant, because only one personnel shift—with no overtime—would now be required in a tissue bank, reducing the costs involved and enabling the same person to perform the whole protocol for consistency purposes although it is acknowledged that significant preparation work would need to be performed by another staff member prior to the actual vitrification process. The optimization of the protocol thus encourages clinical use of articular cartilage vitrification previously shown to be effective at preserving some cell viability [20].

Author contributions

Experimental design: JAWE, LEM, NMJ
Performance of experiment: KKA, HY
Computational study design: NS, JAWE, NMJ
Performance of computational study: NS
Evaluation of results: NS, KKA, HY, JAWE, LEM, NMJ
Writing and review of manuscript: NS, KKA, HY, JAWE, LEM, NMJ

Conflict of interest statement

Authors NMJ, LEM, and JAWE are inventors on US Patent No. 8,758,988, N.M. Jomha, L.E. McGann, J.A.W. Elliott, G. Law, F. Forbes, A. Torghabeh Abazari, B. Maghdoori and A. Weiss, “Cryopreservation of articular cartilage”.

Acknowledgements

Funding was provided by the Canadian Institutes for Health Research (CIHR 93805), Edmonton Orthopaedic Research Committee and the Natural Sciences and Engineering Research Council (NSERC) of Canada. JAWE holds a Canada Research Chair in Thermodynamics.

References

[1] A. Abazari, J.A.W. Elliott, L.E. McGann, R.B. Thompson, MR spectroscopy measurement of the diffusion of dimethyl sulfoxide in articular cartilage and comparison to theoretical predictions, Osteoarthr. Cartil. 20 (2012) 1004–1010.
[2] A. Abazari, J.A.W. Elliott, G.K. Law, L.E. McGann, N.M. Jomha, A biomechanical triphasic approach to the transport of nondilute solutions in articular cartilage, Biophys. J. 97 (2009) 3054–3064.
[3] A. Abazari, N.M. Jomha, J.A.W. Elliott, L.E. McGann, Review: Cryopreservation of articular cartilage, Cryobiology 66 (2013) 201–209.
[4] A. Abazari, N.M. Jomha, G.K. Law, J.A.W. Elliott, L.E. McGann, Erratum to ‘Permeation of several cryoprotectants in porcine articular cartilage’ [Cryobiology 58 (2009) 110–114], Cryobiology 59 (2009) 369.
[5] A. Abazari, R.B. Thompson, J.A.W. Elliott, L.E. McGann, Transport phenomena in articular cartilage cryopreservation as predicted by the modified triphasic model and the effect of natural inhomogeneities, Biophys. J. 102 (2012) 1284–1293.
[6] K.A. Almansoori, V. Prasad, J.F. Forbes, G.K. Law, L.E. McGann, J.A.W. Elliott, N.M. Jomha, Cryoprotective agent toxicity interactions in human articular chondrocytes, Cryobiology 64 (2012) 185–191.
[7] P.P. Aubin, H.K. Cheah, A.M. Davis, A.E. Gross, Long-term followup of fresh femoral osteochondral allografts for posttraumatic knee defects, Clin. Orthop. 391 (2001) S318–S327.
[8] S.T. Ball, D. Amiel, S.K. Williams, W. Tontz, A.C. Chen, R.L. Sah, W.D. Bugbee, The effects of storage on fresh human osteochondral allografts, Clin. Orthop. 418 (2004) 246–252.
[9] K.G.M. Brockbank, Z.Z. Chen, Y.C. Song, Vitrification of porcine articular cartilage, Cryobiology 60 (2010) 217–221.
[10] J. Crank, The Mathematics of Diffusion, second ed., Clarendon Press, Oxford, 1975.
[11] D.P. Eisenberg, M.J. Taylor, Y. Rabin, Thermal expansion of the cryoprotectant cocktail DP6 combined with synthetic ice modulators in presence and absence of biological tissues, Cryobiology 65 (2012) 117–125.
[12] J.A.W. Elliott, R.C. Prickett, H.Y. Elmoazzen, K.R. Porter, L.E. McGann, A multisolute osmotic virial equation for solutions of interest in biology, J. Phys. Chem. B 111 (2007) 1775–1785.
[13] G.M. Fahy, D.R. MacFarlane, C.A. Angell, H.T. Meryman, Vitrification as an approach to cryopreservation, Cryobiology 21 (1984) 407–426.
[14] T.M. Farooque, Z. Chen, Z. Schwartz, T.M. Wick, B.D. Boyan, K.G.M. Brockbank, Protocol development for vitrification of tissue-engineered cartilage, Bioprocessing (Williamsbg Va) 8 (2009) 29–36.
[15] S. Gortz, W.D. Bugbee, Allografts in articular cartilage repair, J. Bone Jt. Surg. Am. 88 (2006) 1374–1384.
[16] L. Hangody, P. Feczko, L. Bartha, G. Bodo, G. Kish, Mosaicplasty for the treatment of articular defects of the knee and ankle, Clin. Orthop. 391 (2001) S328–S336.
[17] K. Hjelle, E. Solheim, T. Strand, R. Muri, M. Brittberg, Articular cartilage defects in 1,000 knee arthroscopies, Arthroscopy 18 (2002) 730–734.
[18] N.M. Jomha, P.C. Anoop, L.E. McGann, Intramatrix events during cryopreservation of porcine articular cartilage using rapid cooling, J. Orthop. Res. 22 (2004) 152–157.
[19] N.M. Jomha, G. Lavoie, K. Muldrew, N.S. Schachar, L.E. McGann, Cryopreservation of intact human articular cartilage, J. Orthop. Res. 20 (2002) 1253–1255.
[20] N.M. Jomha, J.A.W. Elliott, G.K. Law, B. Maghdoori, J. Fraser Forbes, A. Abazari, A.B. Adesida, L. Laouar, X. Zhou, L.E. McGann, Vitrification of intact human articular cartilage, Biomaterials 33 (2012) 6061–6068.
[21] N.M. Jomha, G.K. Law, A. Abazari, K. Rekieh, J.A.W. Elliott, L.E. McGann, Permeation of several cryoprotectant agents into porcine articular cartilage, Cryobiology 58 (2009) 110–114.
[22] N.M. Jomha, A.D.H. Weiss, J. Fraser Forbes, G.K. Law, J.A.W. Elliott, L.E. McGann, Cryoprotectant agent toxicity in porcine articular chondrocytes, Cryobiology 61 (2010) 297–302.
[23] L.L. Kuleshova, S.S. Gouk, D.W. Hutmacher, Vitrification as a prospect for cryopreservation of tissue-engineered constructs, Biomaterials 28 (2007) 1585–1596.
[24] A. Lawson, I.N. Mukherjee, A. Sambanis, Mathematical modeling of cryoprotectant addition and removal for the cryopreservation of engineered or natural tissues, Cryobiology 64 (2012) 1–11.
[25] G.A. Matricali, G. Dereymaeker, F.P. Luyten, Donor site morbidity after articular cartilage repair procedures: a review, Acta Orthop. Belg. 76 (2010) 669–674.
[26] I.N. Mukherjee, Y. Li, Y.C. Song, R.C. Long, A. Sambanis, Cryoprotectant transport through articular cartilage for long-term storage: experimental and modeling studies, Osteoarthr. Cartil. 16 (2008) 1379–1386.
[27] D.A. Noday, P.S. Steif, Y. Rabin, Viscosity of cryoprotective agents near glass transition: a new device, technique, and data on DMSO, DP6, and VS55, Exp. Mech. 49 (2009) 663–672.
[28] C. Ohlendorf, W.W. Tomford, H.J. Mankin, Chondrocyte survival in cryopreserved osteochondral articular cartilage, J. Orthop. Res. 14 (1996) 413–416.
[29] D.E. Pegg, The relevance of ice crystal formation for the cryopreservation of tissues and organs, Cryobiology 60 (2010) S36–S44.
[30] R.C. Prickett, J.A.W. Elliott, L.E. McGann, Application of the osmotic virial equation in cryobiology, Cryobiology 60 (2010) 30–42.
[31] R. Sharma, G.K. Law, K. Rekieh, A. Abazari, J.A.W. Elliott, L.E. McGann, N.M. Jomha, A novel method to measure cryoprotectant permeation into intact articular cartilage, Cryobiology 54 (2007) 196–203.
[32] S.D. Taylor, E. Tsiridis, E. Ingham, Z.M. Jin, J. Fisher, S. Williams, Comparison of human and animal femoral head chondral properties and geometries, Proc. Inst. Mech. Eng. H J. Eng. Med. 226 (2012) 55–62.
[33] A.D.H. Weiss, J. Fraser Forbes, A. Scheuerman, G.K. Law, J.A.W. Elliott, L.E. McGann, N.M. Jomha, Statistical prediction of the vitrifiability and glass stability of multi-component cryoprotective agent solutions, Cryobiology 61 (2010) 123–127.
[34] R.J. Williams, J.C. Dreese, C.T. Chen, Chondrocyte survival and material properties of hypothermically stored cartilage – an evaluation of tissue used for

osteochondral allograft transplantation, Am. J. Sports Med. 32 (2004) 132–139.
[35] B. Wowk, Thermodynamic aspects of vitrification, Cryobiology 60 (2010) 11–22.
[36] H. Yu, K. Al-Abbasi, J.A.W. Elliott, L.E. McGann, N.M. Jomha, Clinical efflux of cryoprotective agents from vitrified human articular cartilage, Cryobiology 66 (2013) 121–125.
[37] M.W. Zielinski, L.E. McGann, J.A. Nychka, J.A.W. Elliott, Comparison of non-ideal solution theories for multi-solute solutions in cryobiology and tabulation of required coefficients, Cryobiology 69 (2014) 305–317.